

# Di(*tert*-butyl)phosphate Complexes of Aluminum: Precursors to Aluminum Phosphate Xerogels and Thin Films

Claus G. Lugmair,<sup>†,‡</sup> T. Don Tilley,<sup>\*,†,‡</sup> and Arnold L. Rheingold<sup>\*,§</sup>

Contribution from the Department of Chemistry, University of California, Berkeley, Berkeley, California 94720-1460, the Chemical Sciences Division, Lawrence Berkeley National Laboratory, 1 Cyclotron Road, Berkeley, California 94720, and the Department of Chemistry and Biochemistry, University of Delaware, Newark, Delaware 19716-2522

Received January 27, 1999. Revised Manuscript Received April 19, 1999

Reactions of  $\text{HO}(\text{O})\text{P}(\text{O}^t\text{Bu})_2$  with  $\text{Al}_2\text{Me}_6$  and  $[\text{Al}(\text{O}^i\text{Pr})_3]_4$  gave the new molecular aluminum phosphate complexes  $[\text{Me}_2\text{AlO}_2\text{P}(\text{O}^t\text{Bu})_2]_2$  (**1**) and  $[\text{Al}(\text{O}^i\text{Pr})_2\text{O}_2\text{P}(\text{O}^t\text{Bu})_2]_4$  (**2**), respectively. In the solid state, **1** exists as a centrosymmetric dimer consisting of two four-coordinate Al centers bridged by two phosphate groups. In the solid state **2** exists as a centrosymmetric tetramer in which the unique half of the tetramer consists of two aluminum atoms bridged by two di(*tert*-butyl)phosphate groups. The central part of the molecule contains a planar  $\text{Al}_2\text{O}_2$  four-membered ring containing two symmetry-related Al(1) atoms bridged by two  $\text{O}^i\text{Pr}$  ligands. Solution-phase thermolyses of **1** and **2** in organic solvents led to the formation of transparent and opaque xerogels, respectively, after air-drying. The xerogel derived from **1** in 2-propanol had a surface area of  $442 \text{ m}^2 \text{ g}^{-1}$  after calcination to  $600^\circ\text{C}$  in air. Thin, transparent films of aluminum phosphate were prepared by chemical vapor deposition (CVD) using both **1** and **2** as molecular precursors.

## Introduction

Aluminophosphates and related materials are useful in a number of applications, in particular as catalysts and catalyst supports.<sup>1</sup> In addition, aluminophosphates have been shown to possess interesting ion exchange and adsorption properties.<sup>2</sup> Considerable attention has focused on the use of sol–gel routes to amorphous aluminophosphates. For stoichiometric  $\text{AlPO}_4$ , aqueous routes have produced materials with surface areas between  $200$  and  $350 \text{ m}^2 \text{ g}^{-1}$ , and gels with surface areas as high as  $565 \text{ m}^2 \text{ g}^{-1}$  have been generated in 2-propanol.<sup>1,3</sup> Aluminophosphate thin films have also attracted attention due to their abrasion resistance, chemical resistance, and low refractive indices.<sup>4a</sup> Films of glassy aluminophosphate have been prepared from solutions of  $\text{AlCl}_3$  and  $\text{H}_3\text{PO}_4$ .<sup>4</sup>

We have previously explored the use of zinc phosphate complexes based on the  $\text{O}_2\text{P}(\text{O}^t\text{Bu})_2$  ligand as precursors to zincophosphate materials.<sup>5</sup> The precursor complex  $\text{Zn}_4(\mu_4\text{-O})[\text{O}_2\text{P}(\text{O}^t\text{Bu})_2]_6$  is thermally labile and is readily converted to a carbon-free zinc phosphate below  $140^\circ\text{C}$  with clean elimination of isobutene and water. In this paper, we describe an extension of this methodology to the preparation of aluminophosphate materials. This work involves synthesis and characterization of the new molecular precursor complexes  $[\text{Me}_2\text{AlO}_2\text{P}(\text{O}^t\text{Bu})_2]_2$  (**1**) and  $[\text{Al}(\text{O}^i\text{Pr})_2\text{O}_2\text{P}(\text{O}^t\text{Bu})_2]_4$  (**2**), and their pyrolytic conversions to materials with very low carbon contents. Preliminary investigations into the utility of these precursors in the synthesis of aluminophosphate materials have shown that thermolyses of **1** and **2** in anhydrous organic solvents lead to high surface area aluminophosphate gels. Also, the volatility of these precursor complexes allows for the fabrication of aluminum phosphate thin films by chemical vapor deposition (CVD).

## Results

**Synthesis and Characterization of Aluminum Phosphate Complexes.** Two equivalents of  $\text{HO}(\text{O})\text{P}(\text{O}^t\text{Bu})_2$ <sup>9</sup> reacted with hexamethyldialuminum in pen-

<sup>†</sup> University of California, Berkeley.

<sup>‡</sup> Lawrence Berkeley National Laboratory.

<sup>§</sup> University of Delaware.

(1) (a) Mostafa, M. R.; Youssef, A. M. *Mater. Lett.* **1998**, *34*, 405. (b) Parida, K.; Mishra, T. *J. Colloid Interface Sci.* **1996**, *179*, 233. (c) Petrakis, D. E.; Hudson, M. J.; Pomonis, P. J.; Sdoukos, A. T.; Bakas, T. V. *J. Mater. Chem.* **1995**, *5*, 1975. (d) Glemza, R.; Parent, Y. O.; Welsh, W. A. *Catal. Today* **1992**, *14*, 175. (e) Costa, A.; Deya, P. M.; Sinisterra, J. V.; Marinas, J. M. *Can. J. Chem.* **1980**, *58*, 1266. (f) Cheung, T. T. P.; Willcox, K. W.; McDaniel, P. M.; Johnson, M. M. *J. Catal.* **1986**, *102*, 10.

(2) (a) Mishra, T.; Parida, K. M.; Rao, S. B. *Sep. Sci. Technol.* **1998**, *33*, 1057. (b) Kandori, K.; Ikeguchi, N.; Yasukawa, A.; Ishikawa, T. *J. Colloid Interface Sci.* **1998**, *202*, 369. (c) Kandori, K.; Ikeguchi, N.; Yasukawa, A.; Ishikawa, T. *J. Colloid Interface Sci.* **1996**, *182*, 425.

(3) Harmer, M. A.; Vega, A. J.; Flippen, R. B. *Chem. Mater.* **1994**, *6*, 1903.

(4) (a) Rotheron, R. N. *Thin Solid Films* **1981**, *77*, 149. (b) Birchall, J. D. *Brit. Ceram. Trans. J.* **1984**, *83*, 158.

(5) Lugmair, C. G.; Tilley, T. D.; Rheingold, A. L. *Chem. Mater.* **1997**, *9*, 339.

(6) Zoellner, R. W. *J. Chem. Educ.* **1990**, *67*, 714.

(7) *Coordination Chemistry of Aluminum*; Robinson, G. H., Ed.; VCH: New York, 1993; p 50.

(8) International Center for Diffraction Data "PC-PDF" **1993**, *2*, Card 11-500.

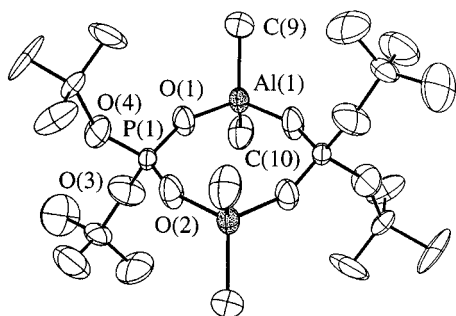
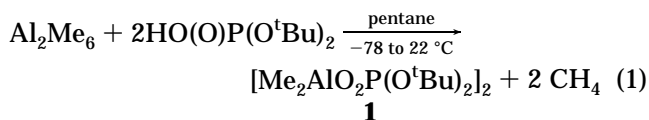


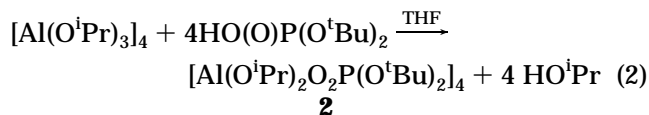
**Figure 1.** ORTEP view of the molecular structure of  $[\text{Me}_2\text{AlO}_2\text{P}(\text{O}^t\text{Bu})_2]_2$  (**1**). Hydrogen atoms were omitted for clarity.

tane at  $-78^\circ\text{C}$  to form  $[\text{Me}_2\text{AlO}_2\text{P}(\text{O}^t\text{Bu})_2]_2$  (**1**) in 90% isolated yield as colorless crystals (eq 1). Addition of 4



equiv of the phosphate to  $\text{Al}_2\text{Me}_6$  also led to the isolation of **1**. A single-crystal X-ray structure analysis revealed that in the solid state, **1** exists as a centrosymmetric dimer (Figure 1). The di(*tert*-butyl)phosphate groups bridge the two Al atoms asymmetrically to form a slightly buckled, eight-membered ring. The short P(1)–O(2) bond of 1.442(4) Å is associated with a long Al(1)–O(2) bond (1.785(4) Å) and the longer P(1)–O(1) bond of 1.463(4) Å is associated with a short Al(1)–O(1) bond (1.767(4) Å). The aluminum atoms are in distorted tetrahedral coordination environments, with bond angles ranging from  $102.8(2)^\circ$  for O(1)–Al(1)–O(2A) to  $118.6(4)^\circ$  for C(9)–Al(1)–C(10).

A more oxygen-rich aluminum phosphate complex, in which the Al atoms are coordinated only by oxygen atoms, was prepared from an aluminum alkoxide. Addition of 4 equiv of  $\text{HO}(\text{O})\text{P}(\text{O}^t\text{Bu})_2$  to a THF solution of  $[\text{Al}(\text{O}^i\text{Pr})_3]_4$  produced  $[\text{Al}(\text{O}^i\text{Pr})_2\text{O}_2\text{P}(\text{O}^t\text{Bu})_2]_4$  (**2**) in 80% isolated yield (eq 2). Use of the alkoxide  $\text{Al}(\text{OEt})_3$  led to many products, while  $\text{Al}(\text{O}^t\text{Bu})_3$  proved to be



unreactive under these conditions. Room-temperature  $^1\text{H}$ ,  $^{13}\text{C}$ , and  $^{31}\text{P}$  NMR spectra of **2** reveal the presence of only one environment for both the  $\text{O}^i\text{Pr}$  and  $\text{O}_2\text{P}(\text{O}^t\text{Bu})_2$  groups. This is consistent with a dimeric structure with terminal  $\text{O}^i\text{Pr}$  and bridging  $\text{O}_2\text{P}(\text{O}^t\text{Bu})_2$  groups. Attempts to determine the solution molecular weight by the Singer method<sup>6</sup> produced inconsistent results due to the slow decomposition of **2** in solution.

Single-crystal X-ray crystallography revealed that in the solid state, **2** is a centrosymmetric tetramer (Figure 2). The unique half of the tetramer consists of two aluminum atoms bridged by two di(*tert*-butyl)phosphate groups to form a boat-shaped eight-membered ring. The central part of the molecule contains a planar  $\text{Al}_2\text{O}_2$  four-membered ring containing two symmetry-related

Al(1) atoms bridged by two  $-\text{O}^i\text{Pr}$  ligands. The Al(2) atoms possess a tetrahedral coordination geometry with O–Al–O bond angles ranging from  $105.1(3)^\circ$  to  $118.1(4)^\circ$ . The five-coordinate Al(1) atom possesses a trigonal-bipyramidal coordination geometry. The O(2)–Al(1)–O(6\*) angle involving the “axial” donor atoms is  $167.1(2)^\circ$ , and the sum of the O–Al–O angles in the “equatorial plane” is  $358.4^\circ$ . The phosphate bridges are distinctly nonsymmetrical. The Al–O bond of the axially bound phosphate is longer (1.896(5) Å) than the equatorially bound phosphate ligand (1.817(5) Å). Similarly, the Al–O bond length of the bridging isopropoxy ligand in the axial position is longer (1.943(5) Å) than the one in the equatorial position (1.798(5) Å). In comparison, the Al–O bond length of the terminal isopropoxy ligand is 1.699(6) Å. The coordination environment of Al(1) is common for five-coordinate Al atoms, which normally possess trigonal-bipyramidal coordination with covalently bound ligands in the equatorial positions and datively bound ligands in the axial positions.<sup>7</sup>

**Ceramic Conversions of the Precursor Complexes 1 and 2.** The thermal gravimetric analysis (TGA) trace for complex **1** (Figure 3) corresponds to a precipitous weight loss with an onset temperature of  $\sim 150^\circ\text{C}$  and a ceramic yield of 42.0% at  $500^\circ\text{C}$ . The latter value is slightly lower than the calculated ceramic yield for  $\text{AlPO}_4$  of 45.8%. During the decomposition of **1**, a liquid formed (at  $\sim 166^\circ\text{C}$ ), which became an insoluble solid upon further heating. The DSC curve for **1** reveals two endothermic transitions at  $136^\circ\text{C}$  and  $171^\circ\text{C}$ . There are also three exotherms at 183, 191, and  $197^\circ\text{C}$ , associated with decomposition. When carefully heated under reduced pressure, **1** sublimed ( $100^\circ\text{C}$ , 0.001 mmHg) with only minor decomposition. The volatile decomposition products were collected by vacuum transfer and identified by  $^1\text{H}$  NMR spectroscopy using ferrocene as an internal standard. Only isobutene and methane were detected as volatile decomposition products. The solid-state material produced by thermolysis of **1** to  $300^\circ\text{C}$  in air, followed by heating to  $1400^\circ\text{C}$  under  $\text{N}_2$ , exhibited a broad, low-intensity peak at  $\sim 22^\circ 2\theta$  in the XRD powder pattern, consistent with poorly crystalline, orthorhombic  $\text{AlPO}_4$ .<sup>8</sup> The DTA curve for **1** contains a small exothermic transition at  $1150^\circ\text{C}$  possibly due to the crystallization of this phase.

The decomposition of **2** begins near room temperature (by TGA). Weight loss is gradual until  $140^\circ\text{C}$ , at which point the weight loss becomes rapid (Figure 4). At  $1000^\circ\text{C}$ , the ceramic yield is 35.8%, which is close to the yield expected for  $\text{AlPO}_4$  (34.4%). Upon heating, **2** also produced an oil as it decomposed (at  $\sim 150^\circ\text{C}$ ). Complex **2** can be sublimed at  $80^\circ\text{C}$  and  $<0.001$  mmHg, with only minor decomposition. The volatile decomposition products were isobutene, propene,  $\text{HO}^i\text{Pr}$ , and water, in a 1:0.3:1.1:0.67 ratio. The solid-state material produced by thermolysis of **2** to  $300^\circ\text{C}$  in air and then to  $1400^\circ\text{C}$  under  $\text{N}_2$  had a broad low intensity peak at  $\sim 22^\circ 2\theta$  in the XRD powder pattern consistent with very poorly crystalline, orthorhombic  $\text{AlPO}_4$ .<sup>8</sup>

**Compounds 1 and 2 as Precursors for CVD Thin-Film Growth.** The volatility of **1** and **2** provided the opportunity to prepare aluminum phosphate thin films by chemical vapor deposition (CVD). The CVD apparatus employed consisted of a Pyrex tube, closed at

(9) International Center for Diffraction Data “PC-PDF” 1993, 2, Card 20-44.

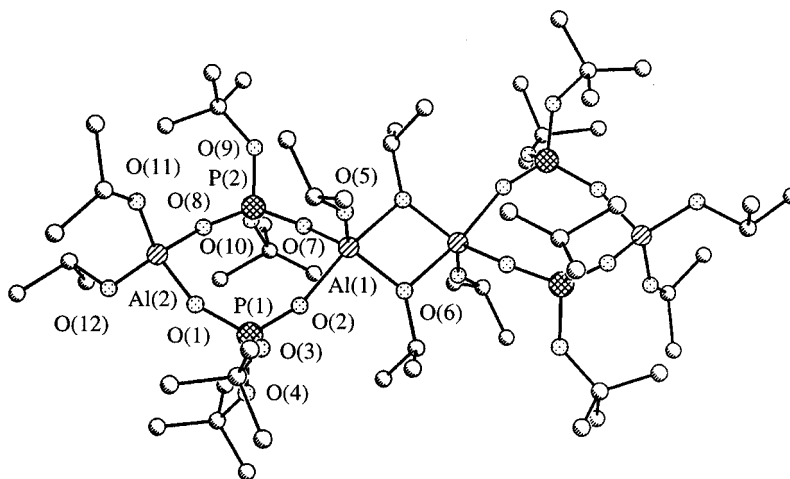


**Figure 2.** Spherical atom drawing of the molecular structure of  $[\text{Al}(\text{O}^i\text{Pr})_2\text{O}_2\text{P}(\text{O}^t\text{Bu})_2]_4$  (**2**). Hydrogen atoms were omitted for clarity.

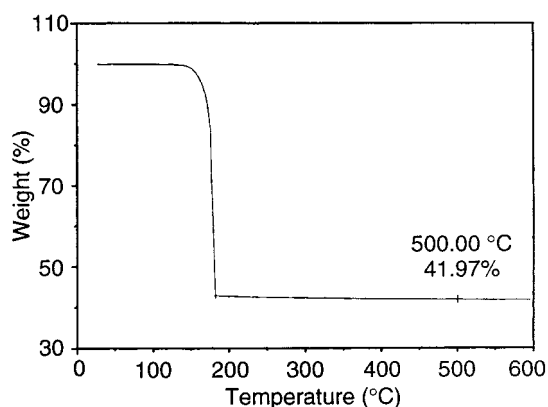


**Figure 3.** TGA trace for **1** under  $\text{N}_2$ , with a heating rate of  $10^\circ\text{C min}^{-1}$ .

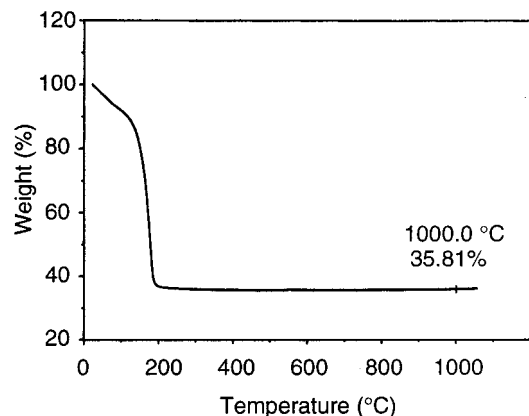


**Figure 4.** TGA trace for **2** under  $\text{N}_2$ , with a heating rate of  $10^\circ\text{C min}^{-1}$ .

one end and equipped at the other end with a valve to a high vacuum line. The precursor ( $\sim 0.2$  g) was placed in the closed end of the tube, glass slides were placed in the center of the tube, and a dynamic vacuum was applied (0.001 mmHg). The sealed end of the tube was then gently heated ( $100^\circ\text{C}$ ) to volatilize the precursor, after the rest of the tube had been preheated to  $200^\circ\text{C}$  with heating tape. As the precursor came into contact with the hot glass slides and tube walls, it deposited a colorless, transparent film. After about 2 h of film growth and cooling of the apparatus to room temperature, thicker regions of the films cracked and partially

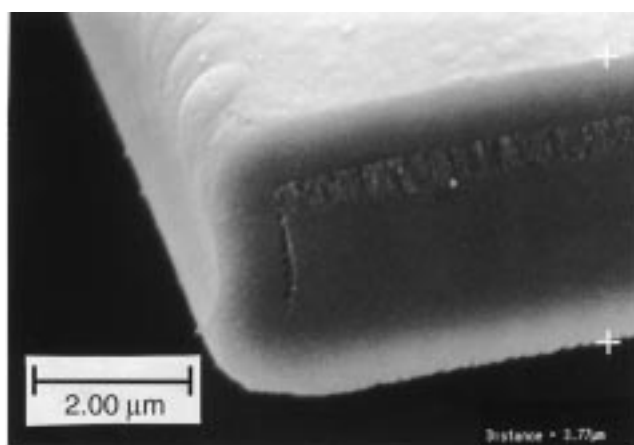


**Figure 5.** Scanning electron micrograph of the thin film grown by CVD from **1**.

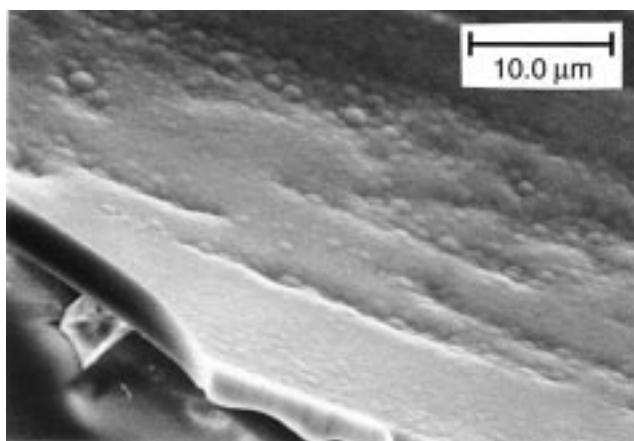


**Figure 6.** Scanning electron micrograph of the thin film grown by CVD from **2**.

peeled away from the glass, whereas thinner regions of the film remained intact. Figure 5 shows a scanning electron micrograph of the aluminophosphate film derived from **1**. The film is about  $3\ \mu\text{m}$  thick, is nonporous, and has a slightly lumpy surface topology. Figure 6 provides a scanning electron micrograph of the thin film derived from **2**, viewed from an edge. In this case the film thickness is about  $4\ \mu\text{m}$ , and the surfaces exposed during film growth are somewhat lumpy. The Al:P:O ratio of the film derived from **2** is 1.00:0.99:4.27 as



determined by electron microprobe analysis. Combustion analysis reveals that the film derived from **2** contains only 0.37% carbon and 2.04% hydrogen.

**Solution-Phase Pyrolytic Transformation of 1 and 2 to  $\text{AlPO}_4$  Xerogels.** The solubility of **1** and **2** in organic solvents, and their low-temperature thermolysis, suggested their use as single-source precursors to aluminum phosphate gels via nonhydrolytic, pyrolytic transformations.

Gels of **1** were prepared by heating toluene or 2-propanol solutions of the precursor to 140 °C for ~12 h in a sealed glass ampule. From toluene, a gel monolith was formed, which shrunk by ~40% without cracking upon air-drying over 3 days. The dry gel monolith was hard and transparent. After calcination to 300 °C in air for 1 h, the surface area of the gel was 165 m<sup>2</sup> g<sup>-1</sup> (single-point BET analysis). Combustion analysis revealed that this material contains 1.03% carbon and 2.34% hydrogen. Further calcination to 600 °C in air for 30 min resulted in an increase in the surface area to 320 m<sup>2</sup> g<sup>-1</sup>, and a gel that was amorphous by XRD. Further calcination to 1200 °C for 2 h under O<sub>2</sub> resulted in crystallization of the tridymite form of  $\text{AlPO}_4$ .<sup>9</sup> Upon air-drying, the gel prepared from 2-propanol crumbled to small pieces which appeared transparent when viewed under an optical microscope. This xerogel retains a large amount of solvent, as indicated by TGA analysis, which revealed a 30% weight loss to 200 °C and thereafter a steady, slow weight loss of an additional 3.6% to 1000 °C. This xerogel had a surface area of 386 m<sup>2</sup> g<sup>-1</sup> after calcination to 300 °C for 30 min and contained only 0.37% carbon and 2.60% hydrogen by combustion analysis. Further calcination to 600 °C in air for 30 min resulted in an increase in surface area to 442 m<sup>2</sup> g<sup>-1</sup>. The latter sample was amorphous after calcination to 600 °C and crystallized to the tridymite form of  $\text{AlPO}_4$  at 1200 °C under O<sub>2</sub>.

Xerogels were also obtained from **2** in toluene and 2-propanol solvents. In both cases, clear "wet" gels were obtained after heating the solutions to 145 °C for 15 h. Both samples turned opaque and white upon air-drying, and their volumes were reduced by ~70%. The dry materials appeared as agglomerated spherical particles under an optical microscope. The gel powder prepared in 2-propanol had a BET surface area of 242 m<sup>2</sup> g<sup>-1</sup> after calcination to 300 °C in air for 1 h, and a surface area of 288 m<sup>2</sup> g<sup>-1</sup> after calcination to 600 °C in air for 1 h. The gel prepared in toluene had a BET surface area of 92 m<sup>2</sup> g<sup>-1</sup> after calcination to 300 °C in air for 1 h and a surface area of 83 m<sup>2</sup> g<sup>-1</sup> after calcination to 600 °C in air for 1 h. After calcination to 600 °C, this material contained 0.44% carbon and 2.30% hydrogen by combustion analysis. Both samples were amorphous (by XRD) after calcination to 600 °C, and both samples contained the tridymite form of  $\text{AlPO}_4$ <sup>9</sup> after calcination to 1200 °C.

## Discussion

The aluminum phosphate complexes **1** and **2** can be prepared in high yield (≥90%). In both complexes the phosphate groups bridge between two aluminum centers rather than chelating to one aluminum center. This structural feature is not unexpected, as the absence of chelating phosphate groups has been attributed to the

steric strain that would be present in the four-membered chelate ring.<sup>10</sup> The  $\text{Al}_2\text{P}_2\text{O}_4$  rings present in **1** and **2** are a common structural feature also seen in the related compound  $[\text{tBu}_2\text{AlO}_2\text{P}(\text{OSiMe}_3)_2]_2$ <sup>11a</sup> and in numerous gallophosphates and gallophosphonates.<sup>11</sup> Many phosphonate clusters also contain  $\text{M}_2\text{P}_2\text{O}_4$  rings.<sup>12</sup> The solid-state decompositions of **1** and **2** are marked by a precipitous weight loss at low temperatures, between 150 and 200 °C. Interestingly, **1** shows no sign of decomposition below the temperature at which sudden decomposition occurs, whereas **2** decomposes slowly just above room temperature. This appears to reflect a greater thermal stability for aluminum alkyls vs aluminum alkoxides in this system.

The volatility of both **1** and **2** make these complexes good reagents for the chemical vapor deposition (CVD) of aluminum phosphate thin films. Thin films (≤1 μm) prepared from these complexes at 200 °C were smooth, dense, and transparent. Under these nonoptimized conditions, thicker films partially cracked and peeled from the substrate. This occurred only near the center of the film, where it is thickest. Previously, aluminophosphate thin films were prepared from solutions of  $\text{AlCl}_3$  and  $\text{H}_3\text{PO}_4$ .<sup>4</sup> The CVD route described here is complementary to the latter method, as it can be used to form films on substrates that are sensitive to strong acids.

The solution-phase thermolyses of **1** and **2** gave gels with significantly different properties. The xerogels derived from **1** were colorless and transparent, while those prepared from **2** were opaque and white. Calcination of the gel prepared from **1** in 2-propanol at 600 °C led to a material with a high surface area (442 m<sup>2</sup> g<sup>-1</sup>). In comparison, aluminophosphate gels prepared by aqueous sol-gel routes have surface areas between 200 and 350 m<sup>2</sup> g<sup>-1</sup>,<sup>1d,3</sup> while gels prepared in 2-propanol using aluminum alkoxides have surface areas up to 565 m<sup>2</sup> g<sup>-1</sup>.<sup>3</sup>

## Experimental Section

All manipulations were performed under a nitrogen atmosphere using standard Schlenk techniques or a Vacuum Atmospheres drybox. Tetrahydrofuran and pentane were distilled from sodium benzophenone under nitrogen. Toluene and 2-propanol were distilled from sodium under nitrogen and then degassed. NMR spectra were recorded on a Bruker AMX-300 spectrometer at 300 (1H), 75.5 (13C), or 121.5 (31P) MHz, or on a Bruker AMX-400 spectrometer at 400 (1H), 100 (13C), or 161 (31P) MHz. Benzene-*d*<sub>6</sub>, vacuum transferred from Na/K alloy, was used as the solvent for all NMR studies. Infrared spectra were collected as Nujol mulls on a Mattson Galaxy 3000 spectrometer, using CsI cells. Thermolyses were performed using a Lindberg 1700 °C furnace, or a Lindberg 1200 °C three-zone tube furnace. Thermal analyses were performed on a DuPont model 2000 thermal analysis system. Powder X-ray diffraction was performed on a Siemens D5000 spectrometer. Scanning electron microscopy was performed on a

(10) Karayannis, N. M.; Mikulski, C. M.; Pytlewski, L. L. *Inorg. Chim. Acta Rev.* **1971**, 69.

(11) (a) Mason, M. R.; Matthews, M. R.; Mashuta, M. S.; Richardson, J. F. *Inorg. Chem.* **1996**, 35, 5756. (b) Mason, M. R.; Perkins, A. M.; Matthews, R. M.; Fisher, J. D.; Mashuta, M. S.; Vij, A. *Inorg. Chem.* **1998**, 37, 3734. (c) Mason, M. R.; Mashuta, M. S.; Richardson, J. F. *Angew. Chem., Int. Ed. Engl.* **1997**, 36, 239. (d) Keys, A.; Bott, S.; Barron, A. R. *J. Chem. Soc., Chem. Commun.* **1996**, 2339.

(12) (a) Walawalker, M. G.; Roesky, H. W.; Murugavel, R. *Acc. Chem. Rev.* **1999**, 32, 117. (b) Walawalker, M. G.; Murugavel, R.; Roesky, H. W.; Usón, I.; Kraetzner, R. *Inorg. Chem.* **1998**, 37, 473.

**Table 1. Selected Interatomic Distances (Å) and Angles (deg) for [Me<sub>2</sub>AlO<sub>2</sub>P(O<sup>t</sup>Bu)<sub>2</sub>]<sub>2</sub> (1)**

(a) Bond Distances			
P(1)–O(2)	1.442(4)	P(1)–O(1)	1.463(4)
P(1)–O(4)	1.482(5)	P(1)–O(3)	1.497(5)
Al(1)–O(1)	1.767(4)	Al(1)–O(2*)	1.785(4)
Al(1)–C(10)	1.919(7)	Al(1)–C(9)	1.947(7)
O(2)–Al(1*)	1.785(4)	O(3)–C(1)	1.393(8)
O(4)–C(5)	1.383(8)		
(b) Bond Angles			
O(2)–P(1)–O(1)	113.9(3)	O(2)–P(1)–O(4)	108.4(4)
O(1)–P(1)–O(4)	110.8(3)	O(2)–P(1)–O(3)	113.7(4)
O(1)–P(1)–O(3)	106.5(3)	O(4)–P(1)–O(3)	102.9(4)
O(1)–Al(1)–O(2*)	102.8(2)	O(1)–Al(1)–C(10)	111.1(3)
O(2*)–Al(1)–C(10)	108.2(3)	O(1)–Al(1)–C(9)	106.7(3)
O(2*)–Al(1)–C(9)	108.3(3)	C(10)–Al(1)–C(9)	118.6(4)
P(1)–O(1)–Al(1)	156.6(3)	P(1)–O(2)–Al(1*)	156.7(3)
C(1)–O(3)–P(1)	144.4(7)	C(5)–O(4)–P(1)	148.4(5)

Cambridge 360 scanning electron microscope. The electron microprobe analysis was performed by John Donovan on a Cameca SX-51 using custom software in the Department of Geology and Geophysics at the University of California, Berkeley. The compounds Al<sub>2</sub>Me<sub>6</sub> (neat) and [Al(O<sup>i</sup>Pr)<sub>3</sub>]<sub>4</sub> were purchased from Aldrich. The latter was distilled before use. The compound H(O)P(O<sup>t</sup>Bu)<sub>2</sub><sup>13</sup> was prepared according to literature procedures.

**[Me<sub>2</sub>AlO<sub>2</sub>P(O<sup>t</sup>Bu)<sub>2</sub>]<sub>2</sub> (1).** A pentane solution (20 mL) of HO(O)P(O<sup>t</sup>Bu)<sub>2</sub> (1.00 g, 4.76 mmol) was added dropwise to a pentane solution (20 mL) of Al<sub>2</sub>Me<sub>6</sub> (0.46 mL, 2.38 mmol) that was precooled to –78 °C. The reaction mixture was allowed to warm to room temperature over 1 h. Stirring was continued for an additional 3 h. The solvent was removed in vacuo, and the remaining white solid was dissolved in pentane (15 mL). The solution was filtered, concentrated to 5 mL, and cooled to –40 °C to afford colorless crystals of **1** (1.15 g) in 90% yield. <sup>1</sup>H NMR (300 MHz): δ 1.31 (s, 36 H, POC(CH<sub>3</sub>)<sub>3</sub>), –0.29 (s, 12 H, AlCH<sub>3</sub>). <sup>13</sup>C{<sup>1</sup>H} NMR (75.5 MHz): δ 83.22 (d, <sup>2</sup>J<sub>CP</sub> = 6.3 Hz), 29.66 (d, <sup>3</sup>J<sub>CP</sub> = 3.5 Hz), –9.02 (s). <sup>31</sup>P{<sup>1</sup>H} NMR (121.5 MHz): δ –22.57 (s). IR (Nujol, CsI, cm<sup>–1</sup>): 1396 w, 1373 m, 1255 m, 1217 s, 1187 m sh, 1097 s, 1049 s, 1026 s sh, 921 w, 833 w, 819 w sh, 683 s, 564 w, 544 w sh, 512 w sh, 487 w sh, 471 w, 444 m, 421 m. Anal. Calcd. for C<sub>20</sub>H<sub>48</sub>Al<sub>2</sub>O<sub>8</sub>P<sub>2</sub>: C, 45.11; H, 9.09; P, 11.63. Found: C, 45.25; H, 9.09; P, 11.80. Selected interatomic distances and angles for **1** are given in Table 1.

**[Al(O<sup>i</sup>Pr)<sub>2</sub>O<sub>2</sub>P(O<sup>t</sup>Bu)<sub>2</sub>]<sub>4</sub> (2).** A THF solution (50 mL) of HO(O)P(O<sup>t</sup>Bu)<sub>2</sub> (5.20 g, 24.7 mmol) was added dropwise to an ice-cold THF solution (50 mL) of [Al(O<sup>i</sup>Pr)<sub>3</sub>]<sub>4</sub> (5.05 g, 6.18 mmol). The reaction mixture was allowed to warm to room temperature over 2 h and was then stirred for 12 h. The solvent was removed under reduced pressure to leave a white solid. The solid was extracted with pentane (40 mL), and the combined extracts were concentrated to 30 mL and cooled to –40 °C to afford colorless crystals of **2** (7.93 g) in 91% yield. <sup>1</sup>H NMR (300 MHz): δ 4.50 (sept, *J* = 6.0 Hz, OCH(CH<sub>3</sub>)<sub>2</sub>), 1.44 (d, <sup>4</sup>J<sub>PH</sub> = 0.6 Hz), 1.435 (d, *J* = 6.0 Hz, OCH(CH<sub>3</sub>)<sub>2</sub>). <sup>13</sup>C{<sup>1</sup>H} NMR (75.5 MHz): δ 84.40 (d, <sup>2</sup>J<sub>CP</sub> = 7.9 Hz), 63.62 (s), 29.67 (d, <sup>3</sup>J<sub>CP</sub> = 4.3 Hz), 28.35 (s). <sup>31</sup>P{<sup>1</sup>H} NMR (121.5 MHz): δ –24.87 (s). IR (Nujol, CsI, cm<sup>–1</sup>): 1460 m, 1395 w, 1369 s, 1251 s, 1169 s, 1290 s, 1059 m sh, 1040 s, 1012 s, 959 m sh, 920 w, 854 w sh, 835 m, 819 w sh, 718 s, 678 m, 657 w sh, 634 vw sh, 611 m, 552 m, 532 m, 485 s, 460 m, 442 w sh, 408 w. Anal. Calcd. for C<sub>14</sub>H<sub>32</sub>AlO<sub>6</sub>P: C, 47.45; H, 9.10. Found: C, 47.19; H, 8.93. Selected interatomic distances and angles for **2** are given in Table 2.

**Thin Films from 1 and 2 by CVD.** The CVD apparatus was a horizontally mounted Pyrex tube that was sealed at one end. The open end of the tube was connected through a valve to a high vacuum line. The tube was charged with either **1** or **2** (~0.2 g) at the sealed end of the tube. Glass microscope slides were placed near the center of the tube. The system was then placed under dynamic vacuum (~0.001 mmHg). At lower

**Table 2. Selected Interatomic Distances (Å) and Angles (deg) for [Al(O<sup>i</sup>Pr)<sub>2</sub>O<sub>2</sub>P(O<sup>t</sup>Bu)<sub>2</sub>]<sub>4</sub> (2)<sup>a</sup>**

(a) Bond Distances			
P(1)–O(2)	1.467(5)	P(1)–O(1)	1.496(5)
P(1)–O(4)	1.508(7)	P(1)–O(3)	1.539(7)
P(2)–O(8)	1.465(6)	P(2)–O(7)	1.483(5)
P(2)–O(10)	1.492(7)	P(2)–O(9)	1.520(6)
Al(1)–O(5)	1.699(6)	Al(1)–O(6)	1.798(5)
Al(1)–O(7)	1.817(5)	Al(1)–O(2)	1.896(5)
Al(1)–O(6*)	1.943(5)	Al(1)–Al(1*)	2.950(4)
Al(2)–O(11)	1.673(8)	Al(2)–O(12)	1.693(7)
Al(2)–O(1)	1.754(5)	Al(2)–O(8)	1.755(6)
O(6)–Al(1*)	1.943(5)		
(b) Bond Angles			
O(2)–P(1)–O(1)	115.6(3)	O(2)–P(1)–O(4)	111.6(4)
O(1)–P(1)–O(4)	112.3(4)	O(2)–P(1)–O(3)	105.4(4)
O(1)–P(1)–O(3)	109.3(4)	O(4)–P(1)–O(3)	101.4(5)
O(8)–P(2)–O(7)	115.2(3)	O(8)–P(2)–O(10)	107.5(5)
O(7)–P(2)–O(10)	111.4(4)	O(8)–P(2)–O(9)	110.6(4)
O(7)–P(2)–O(9)	107.2(3)	O(10)–P(2)–O(9)	104.3(5)
O(5)–Al(1)–O(6)	121.6(3)	O(5)–Al(1)–O(7)	116.3(3)
O(6)–Al(1)–O(7)	120.5(3)	O(5)–Al(1)–O(2)	98.9(3)
O(6)–Al(1)–O(2)	94.2(2)	O(7)–Al(1)–O(2)	89.3(2)
O(5)–Al(1)–O(6*)	93.4(3)	O(6)–Al(1)–O(6*)	76.0(2)
O(7)–Al(1)–O(6*)	88.7(2)	O(2)–Al(1)–O(6*)	167.1(2)
O(11)–Al(2)–O(1)	112.3(4)	O(11)–Al(2)–O(12)	118.1(4)
O(11)–Al(2)–O(8)	105.7(4)	O(12)–Al(2)–O(1)	106.2(3)
O(1)–Al(2)–O(8)	105.1(3)	O(12)–Al(2)–O(8)	108.7(4)
P(1)–O(2)–Al(1)	158.7(4)	P(1)–O(1)–Al(2)	149.6(4)
C(5)–O(4)–P(1)	138.8(7)	C(1)–O(3)–P(1)	142.3(8)
C(12)–O(6)–Al(1)	135.6(4)	C(9)–O(5)–Al(1)	147.7(8)
Al(1)–O(6)–Al(1*)	104.0(2)	C(12)–O(6)–Al(1*)	120.3(4)
P(2)–O(8)–Al(2)	159.9(5)	P(2)–O(7)–Al(1)	155.2(4)
C(19)–O(10)–P(2)	145.7(7)	C(15)–O(9)–P(2)	135.8(7)
C(26)–O(12)–Al(2)	123.7(7)	C(23)–O(11)–Al(2)	140.6(10)

<sup>a</sup> Symmetry operation used to generate equivalent atoms: (\*) atoms –*x*, –*y* + 2, –*z*.

pressures the precursor sublimes to the cool part of the tube past the hot zone without decomposition. The center of the Pyrex tube was preheated to 200 °C with heating tape. The sealed end of the tube, containing the precursor, was then gently heated (100 °C) to volatilize the precursor. When the precursor came into contact with the hot tube walls it decomposed leaving a colorless, transparent film. The films were grown over ~2 h. The Al:P:O ratio of the film derived from **2** is 1.00:0.99:4.27, as determined by electron microprobe analysis. Combustion analysis found: C, 0.37; H, 2.04.

**Thermolysis of 1 in Solution.** A toluene solution (0.25 mL) or an 2-propanol solution (1.0 mL) of **1** (0.050 g, 0.094 mmol) was sealed in a 10-mL Pyrex tube. The tube was placed in an oven preheated to 140 °C. After the tube was heated for 12 h, a gel monolith had formed. The ampule was cooled and opened, and the gel was allowed to air-dry for 3 days. Calcination of the gel was performed under static air or flowing oxygen (200 cm<sup>3</sup> min<sup>–1</sup>) in a tube furnace.

**Thermolysis of 2 in Solution.** A toluene solution (0.80 mL) or an 2-propanol solution (0.80 mL) of **2** (0.050 g, 0.035 mmol) was sealed in a 10-mL Pyrex tube. The tube was placed in an oven preheated to 145 °C. After the tube was heated for 15 h, white gels had formed in both solvents. The ampule was cooled and opened, and the gel was allowed to air-dry for 3 days. Calcination of the gel was performed under static air in a tube furnace.

**X-ray Crystallography.** Crystallographic data are collected in Table 3. Crystals of **1** were grown from a concentrated pentane solution at –35 °C. The unit cell parameters were obtained by the least-squares refinement of the angular settings of 34 reflections. An absorption correction was not required because the variation in the integrated  $\Psi$ -scan intensities was less than 10%. Systematic absences in the diffraction data uniquely defined the space group as *P2<sub>1</sub>/n*. The structure was solved using direct methods, completed by subsequent difference Fourier synthesis, and refined by full-matrix least-squares procedures. Complex **1** resides on an

**Table 3. Crystallographic Data for Compounds 1, and 2**

compound	1	2
empirical formula	C <sub>20</sub> H <sub>48</sub> Al <sub>2</sub> O <sub>8</sub> P <sub>2</sub>	C <sub>56</sub> H <sub>128</sub> Al <sub>4</sub> O <sub>24</sub> P <sub>4</sub>
formula weight	532.48	1417.38
space group	<i>P</i> 2 <sub>1</sub> / <i>n</i>	<i>P</i> $\bar{1}$
<i>a</i> , Å	10.156(2)	10.614(3)
<i>b</i> , Å	10.342(2)	12.422(4)
<i>c</i> , Å	15.841(3)	17.518(5)
$\alpha$ , $\beta$ , $\gamma$ , deg	90, 98.69(1), 90	90.50(3), 100.66(2), 111.87(1)
volume, Å <sup>3</sup>	1644.7(6)	2099(1)
<i>Z</i>	2	1
$\rho$ (calc), g cm <sup>-3</sup>	1.075	1.121
$\mu$ (Mo K $\alpha$ ), cm <sup>-1</sup>	2.19	1.93
<i>R</i> ( <i>F</i> ), %	7.0	9.2
<i>R</i> ( <i>wF</i> ), %	15.8	21.6
GOF	0.939	1.09

inversion center. Atoms C(6), C(7), and C(8) are equally disordered between two positions. The remaining non-hydrogen atoms were refined anisotropically. Hydrogen atoms were included in idealized positions. All calculations used SHELXTL-PC software (G. Sheldrick, Siemens XRD, Madison, WI).

Crystals of **2** were grown from a concentrated pentane solution at -35 °C. The unit cell parameters were obtained by the least-squares refinement of the angular settings of 36 reflections. An absorption correction was not required because the variation in the integrated  $\Psi$ -scan intensities was less than

10%. Systematic absences in the diffraction data were consistent with the triclinic space groups *P*1 and *P* $\bar{1}$ . The structure was successfully refined in *P*1 to yield chemically reasonable and computationally stable results. The structure was solved using direct methods, completed by subsequent difference Fourier synthesis, and refined by full-matrix least-squares procedures. Complex **2** resides on an inversion center. Atoms C(20), C(21), C(22), C(24), C(25), C(27), and C(28) are equally disordered between two positions. Atoms C(28) and C(29) were refined isotropically. Distances to the disordered atoms in the isopropyl groups were fixed at 1.540 Å. The remaining non-hydrogen atoms were refined anisotropically. Hydrogen atoms were included in idealized positions.

**Acknowledgment.** This work was supported by the Director, Office of Energy Research, Office of Basic Energy Sciences, Chemical Sciences Division, of the U.S. Department of Energy under Contract No. DE-AC03-76SF00098.

**Supporting Information Available:** Tables of atomic coordinates, bond distances and angles, and anisotropic displacement parameters. This material is available free of charge via the Internet at <http://pubs.acs.org>.

CM990057O